Photochemical & Photobiological Sciences

PAPER

Cite this: *Photochem. Photobiol. Sci.*, 2015, **14**, 995

Reaction dynamics of the UV-B photosensor UVR8†

Takaaki Miyamori,[a] Yusuke Nakasone,[a] Kenichi Hitomi,[b] John M. Christie,[b,c] Elizabeth D. Getzoff[b] and Masahide Terazima*[a]

Received 9th January 2015,
Accepted 10th March 2015

DOI: 10.1039/c5pp00012b

www.rsc.org/pps

UVR8 is a recently discovered ultraviolet-B (UV-B) photoreceptor protein identified in plants and algae. In the dark state, UVR8 exists as a homodimer, whereas UV-B irradiation induces UVR8 monomerization and initiation of signaling. Although the biological functions of UVR8 have been studied, the fundamental reaction mechanism and associated kinetics have not yet been fully elucidated. Here, we used the transient grating method to determine the reaction dynamics of UVR8 monomerization based on its diffusion coefficient. We found that the UVR8 photodissociation reaction proceeds in three stages: (i) photoexcitation of cross-dimer tryptophan (Trp) pyramids; (ii) an initial conformational change with a time constant of 50 ms; and (iii) dimer dissociation with a time constant of 200 ms. We identified W285 as the key Trp residue responsible for initiating this photoreaction. Although the C-terminus of UVR8 is essential for biological interactions and signaling *via* downstream components such as COP1, no obvious differences were detected between the photoreactions of wild-type UVR8 (amino acids 1–440) and a mutant lacking the C-terminus (amino acids 1–383). This similarity indicates that the conformational change associated with stage ii cannot primarily be attributed to this region. A UV-B-driven conformational change with a time constant of 50 ms was also detected in the monomeric mutants of UVR8. Dimer recovery following monomerization, as measured by circular dichroism spectroscopy, was decreased under oxygen-purged conditions, suggesting that redox reactivity is a key factor contributing to the UVR8 oligomeric state.

1. Introduction

Plants monitor and respond to the surrounding environment to optimize their growth and survival. Because light is one of the most important environmental factors controlling their development, plants have evolved a variety of photoreceptors to detect light of specific wavelengths. One of these photosensor proteins, UV Resistance Locus 8 (UVR8), has been recently identified from the model flowering plant *Arabidopsis thaliana* as a photoreceptor that responds to ultraviolet-B (UV-B) wavelengths.[1–6] UVR8 was originally identified in a screen for *A. thaliana* mutants hypersensitive to UV-B.[6] Upon UV-B irradiation, UVR8 interacts with downstream signaling components, including Constitutively Photomorphogenic 1 (COP1), to promote photoprotective responses.[2,7–10] UVR8 is unique compared with other photoreceptors, as it does not bind an exogenous chromophore. Instead, UVR8 possesses 14 tryptophans (Trps) capable of absorbing UV-B. Almost all of these Trp residues are conserved in putative UVR8 photoreceptors identified to date from organisms ranging from algae to higher plants.[3,4,8,11] UVR8 exists as a homodimer in the absence of UV-B and monomerizes following photoexcitation.[8,12–15] This photodissociation reaction allows UVR8 to interact with key components such as COP1 to initiate signaling. However, although the biological function of this novel photosensor protein is well studied,[16–28] details of its photoreaction mechanism have yet to be fully elucidated.

Crystal structures of the UVR8 dimer that lack both N- and C-terminal regions of the protein (residues 14–396 and residues 12–381) have been reported.[13,29] According to these structures, the UVR8 monomer has a seven-bladed β-propeller fold resembling that of the human Regulator of Chromatin Condensation 1 (RCC1).[13,30] The UVR8 structure has been considered to be more flexible than RCC1, because the N- and C-terminal β-strands of UVR8 belong to discrete blades of the β-propeller fold, whereas the N- and C-terminal β-strands of RCC1 are linked together within the same blade.[13] The UVR8

[a]*Department of Chemistry, Graduate School of Science, Kyoto University, Oiwake, Kitashirakawa, Sakyo-ku, Kyoto 606-8502, Japan.*
E-mail: mterazima@kuchem.kyoto-u.ac.jp; Fax: +81-75-753-4000;
Tel: +81-75-753-4026
[b]*Department of Integrative Structural and Computational Biology and the Skaggs Institute for Chemical Biology, The Scripps Research Institute, La Jolla, CA 92037, USA*
[c]*Institute of Molecular, Cell and Systems Biology, College of Medical, Veterinary and Life Sciences, Bower Building, University of Glasgow, G12 QQ, UK*
†Electronic supplementary information (ESI) available. See DOI: 10.1039/c5pp00012b

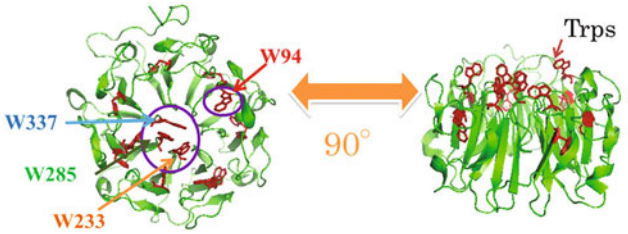

Fig. 1 Structure of UVR8. Tryptophan residues are shown in red. The four labeled tryptophans are considered to be important for UVR8 dissociation.

crystal structures have also revealed that the dimer interface is maintained by ionic interactions between charged amino acids.[13,29] Among the 14 Trps in the UVR8 monomer, six are buried in the protein core and maintain the β-propeller structure, one is located in the C-terminal region absent from the crystal structures, and seven are situated at the homodimeric interface where they are packed with positively charged (basic) residues, mainly arginine and other aromatic residues.[10,11,13,29] In particular, four Trps (W94, W233, W285, and W337) are located adjacent to basic arginine side chains that form cross-dimer salt bridges. These exciton-coupled Trps are arranged to form two "pyramids" across the interface. W285 in particular has been shown to play an important role in UV-B sensing (Fig. 1).[10,11,13,31]

Thus far, UV-driven monomerization of UVR8 has been detected *in vivo* and *in vitro* mostly by biochemical methods, *e.g.*, immunoprecipitation and size exclusion chromatography.[12–15,32] The molecular details underlying the monomerization, however, has not been fully understood. It was originally hypothesized that either cation–Pi interactions between the pyramids Trps and adjacent salt-bridge arginines are disturbed or electron transfer from Trps to neighbouring arginines neutralizes the salt-bridges.[13,29] Ultrafast fluorescence measurements have shown that W285 plays a critical role in primary quenching dynamics in the Trp cluster (~150 ps), most likely in the process of exciton evolution to a charge-separated state to induce the disruption of salt bridges for initiating dimer dissociation.[12] The proposed mechanism has been supported by quantum chemical calculations in which the salt bridges are neutralized by electron and/or proton transfers among W285, R338, W233 and D129.[33,34] Another theoretical study has proposed that the electron transfer between W285 and W233 produces large dipole moment of W233(−)–W285(+) to facilitate the breaking of the cross-dimer salt bridges.[35] All models expect the breakage of salt-bridges would be relevant for the monomerization. A recent FTIR study has directly observed the disruption of the cross-dimer aspartate/arginine salt bridges upon monomerization, which does not accompany major secondary structural change.[36] To date, however, the kinetics of protein conformational change and/or dimer dissociation have not been directly measured, although both are key to understanding the underlying dynamics of the reaction mechanism. In particular, the mechanism by which monomerization occurs has yet to be determined. Furthermore, once dissociated, the UVR8 monomer takes many hours to return to the dimeric form in the absence of UV-B.[13] It is not understood why the dissociated species of UVR8 is so long-lived. To understand the molecular basis underlying these properties, we investigated the reaction dynamics of UVR8.

In this study, we used transient grating (TG) and CD methods to monitor the UVR8 reaction temporally. The TG technique allows the time-resolved detection of reaction dynamics, including association/dissociation events, conformational changes, and higher order (secondary and tertiary) structural changes. Combined with CD measurements, our TG studies indicate that a structural change occurs within the dimer interface prior to photodissociation: this change is also observed in monomeric mutants of UVR8. Among the cross-dimer Trps, W285 is important for instigating the light-driven conformational change associated with UVR8 photoactivation. Moreover, this conformational change is not dependent on the presence of the UVR8 C-terminus.

2. Experimental section

2.1. Sample preparation

All samples used in this study were produced and purified in the same manner as reported in ref. 13. UVR8 was further purified by gel filtration on a Superdex 200 16/60 column (GE Healthcare) and eluted with 25 mM Tris (pH 7.5), 100 mM NaCl, and 1 mM β-mercaptoethanol and concentrated to 10 mg mL^{-1}. Finally, β-mercaptoethanol was removed from the solution by dialysis. Sodium dodecyl sulfate polyacrylamide gel electrophoresis (SDS-PAGE) analysis with and without sample boiling was performed using a narrowband UV-B source as described in ref. 13.

2.2. Measurements

(a) TG method. Principles and experimental protocols of the TG method have been described previously,[37–39] while principles of the analysis are described in ESI (S-1†).[37–39] Briefly, the TG signal was measured using the fourth harmonic of a Nd-YAG laser (266 nm) as the excitation light. The excitation beam was split into two by a beam splitter and focused on a quartz sample cell (2 mm path length) *via* a lens. A blue diode laser beam (449 nm) was used as the probe light. The probe laser beam was brought into the focusing region at the Bragg angle. The diffracted probe beam was detected with a photomultiplier.

Typically, 10–15 signals were averaged by a digital oscilloscope (TDS-7104; Tektronix, Beaverton, OR, USA) to improve the signal/noise ratio. The excitation repetition rate was usually 0.05 Hz, with the sample solution stirred between measurements to avoid excitation of the photoproduct. The laser power for the excitation was set sufficiently low (<40 μJ per pulse) to avoid exciting the photoexcited protein twice by the laser pulse. The q^2-values for each experimental setup

(where q is the grating wavenumber) were determined from the decay rate of the TG signal of the calorimetric reference (aqueous $FeCl_3$ solution). UVR8 protein samples, ranging in concentration from 10 to 100 μM, were used to measure the concentration dependence of the TG signal. Other experiments were performed using a UVR8 concentration of 20 μM for all samples except for W285A, W285F, and D96N/D107N, which were set to 100 μM. All TG measurements were carried out at room temperature.

(b) CD spectral measurements. CD spectra were measured under flowing N_2 gas with a CD spectrometer (J720W1; JASCO, Japan). Protein concentrations ranged from 10 to 20 μM. All samples were measured in a quartz sample cell (2 mm path length) at room temperature. Buffer composition was 50 mM Tris and 150 mM NaCl at pH 7.5. For purging oxygen molecules, N_2 gas was passed over the sample solution at a rate greater than 1 L min^{-1} for 15 min.

3. Results

3.1. Kinetics of the UVR8 photoreaction

The overall time course of the TG signal after photoexcitation of wild-type UVR8 (1–440) at $q^2 = 1.4 \times 10^{11}$ m^{-2} is shown in Fig. 2a. The signal rose quickly within the response time of our system (~30 ns), decayed without recovering to the baseline, and then rose again before finally decaying to the baseline. The rate constants of all components of the TG signal were dependent on q, indicating that these dynamics were representatives of the diffusion process. The initial decay signal was assigned to the thermal grating signal, because its decay rate matched that of a calorimetric reference sample (aqueous $FeCl_3$ solution), which releases all photon energy as heat. (We did not observe any feature indicating the triplet formation and decay processes.) The subsequent rise and decay signals were assigned to molecular diffusion signals. This rise-decay profile indicates a change in diffusion coefficient (D) upon photoexcitation.[37–39] Because the signs of the refractive-index changes are positive for the rise and negative for the decay, the rise and decay kinetics represent the diffusion processes of the product and reactant, respectively. The profile was fitted using the bi-exponential function given in eqn (1) (without the thermal grating term of eqn (S-1) in ESI†):

$$I_{TG}(t) = \alpha\left[-\delta n_R \exp(-D_R q^2 t) + \delta n_P \exp(-D_P q^2 t)\right]^2 \quad (1)$$

(q: grating wavenumber, δn_R: refractive index of the reactant, δn_P: refractive index of the product) The resulting diffusion coefficients of product (D_P) and reactant (D_R) were determined to be 7.1×10^{-11} m^2 s^{-1} and 5.1×10^{-11} m^2 s^{-1}, respectively. (The error of the absolute D value is $\pm 0.3 \times 10^{-11}$ m^2 s^{-1}. However, we can determine the difference between D_P and D_R more accurately, because the signal intensity and the shape is sensitive to the difference; *i.e.*, the error of the relative values between D_P and D_R is much smaller, in this case $\pm 0.1 \times 10^{-11}$ m^2 s^{-1}.) The larger value of D_P relative to D_R indicates that the photoproduct diffused faster than the reactant, consistent with decreased UVR8 size upon photodissociation from dimer to monomer. Assuming that the change in D was due only to the change in volume and both dimer and monomer of UVR8 have (roughly) spherical shapes, the volume ratio of the reactant to the product was calculated according to the Stokes–Einstein relationship (*i.e.*, $\sim[7.1/5.1]^3$) as approximately 2.7, which is larger than the value of 2 expected from the dimer-to-monomer dissociation reaction. (A difference of D between the spherical shape and a slightly ellipsoidal shape is not large.[37,39] Hence, this difference cannot be due to the deviation from the spherical shape.) Consequently, the observed D-change associated with the UVR8 photoreaction may be attributed not only to the dissociation process but also to other phenomena, such as hydrophobic surface exposure during the dissociation as well as a conformational change that will be discussed later.

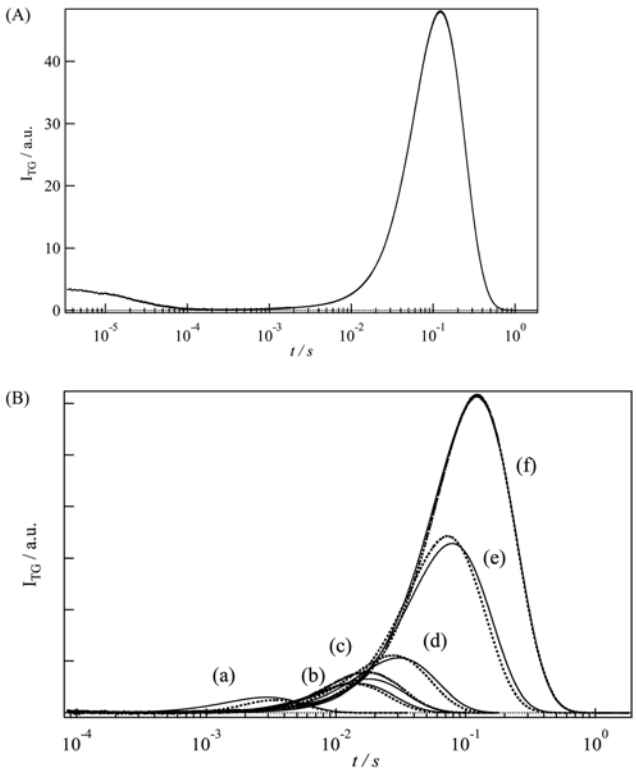

Fig. 2 (A) Typical transient grating (TG) signal after photo-excitation of 20 μM UVR8 at $q^2 = 1.4 \times 10^{11}$ m^{-2}. (B) TG signal q-dependence (dotted lines) at 20 μM for q^2-values of (a) 6.6×10^{12}, (b) 1.3×10^{12}, (c) 1.1×10^{12}, (d) 6.1×10^{11}, (e) 2.3×10^{11}, and (f) 1.4×10^{11} m^{-2}. After normalization to the thermal grating intensity, the signals were fitted (solid lines) by a global analysis with adjustable parameters of the rate constants and diffusion coefficients of the intermediates.

Next, to investigate the dynamics of the reaction, we measured the molecular diffusion signal for various values of q^2 (Fig. 2b). Diffusion signal intensity was strongly dependent on q^2, and increased as the observational time range was extended from a few milliseconds to seconds. This behavior can be qualitatively explained as follows. A weak diffusion

signal intensity was recorded over short observation times: at such times, the change in D between the product and the reactant was small ($D_P \sim D_R$), with the first and second terms in eqn (1) almost cancelling each another out. As the observation time lengthened and the photochemical reaction progressed, D_P, and hence the difference between D_P and D_R, gradually increased, causing the diffusion peak intensity to rise. At longer times (Fig. 2a), the diffusion signal expressed by eqn (1) decayed, indicating that the D-change was almost completed.

Time development of the diffusion signal was first analyzed according to the scheme:

$$R \xrightarrow{h\nu} I \xrightarrow{k} P \quad (2)$$

where R, I, and P denote reactant, intermediate, and product, respectively. The fitting function used is given by eqn (S-4) in ESI.† In this fitting, we used D_P and D_R, as determined above, along with the adjustable parameters D_I and rate constant k. The observed TG signals could not be successfully reproduced using this function, indicating the existence of another reaction dynamic contributing to these diffusion signals. Because the above-mentioned ratio of D_P to D_R suggested a conformational change in addition to the dissociation reaction, we concluded that the additional dynamic was a conformational change. We therefore analyzed the time development of the diffusion signal based on the scheme:

$$R \xrightarrow{h\nu} I_1 \xrightarrow{k_1} I_2 \xrightarrow{k_2} P \quad (3)$$

where I_1 and I_2 are the first and second intermediates. The fitting function used is given by eqn (S-5) in ESI.† Using D_P and D_R obtained above and the adjustable parameters D_{I1} and D_{I2} and rate constants k_1 and k_2, we were able to reasonably reproduce the observed TG signals over a wide range of observation times (100 μs to 1 s) by the global fitting. The time constants of the D-change determined from the fitting were 50 ms and 200 ms, and the D-values of transient intermediates I_1 and I_2 were determined to be 5.1×10^{-11} m^2 s^{-1} and 5.3×10^{-11} m^2 s^{-1}, respectively. (Again, the error of the relative D values is $\pm 0.1 \times 10^{-11}$ m^2 s^{-1}.) The initial reaction ($I_1 \rightarrow I_2$) induced a small change in D (5.1×10^{-11} m^2 s^{-1} → 5.3×10^{-11} m^2 s^{-1}), while the second step ($I_2 \rightarrow P$) led to a larger change (5.3×10^{-11} m^2 s^{-1} → 7.1×10^{-11} m^2 s^{-1}). The small D-change associated with the formation of I_2 (k_1^{-1} = 50 ms) thus most likely reflects the conformational change of UVR8, with the larger D-change in the subsequent process representing the dissociation reaction. The initial conformational change may be a trigger for the dissociation process. The above TG measurements clearly demonstrate that the kinetics of the dissociation and the conformational change can be quantitatively determined by using this method. Furthermore, because the UV-visible absorption spectrum change of UVR8 before and after UV irradiation was negligible, the reaction dynamics could only be detected by monitoring the time development of D, making TG uniquely applicable.

3.2. Dependence on protein concentration and excitation light intensity

Although UVR8 is reported to exist as a dimer in the absence of UV-B,[13,29] an equilibrium between dimeric and monomeric forms might be possible in the resting state. We therefore measured the TG signal at various protein concentrations (from 10 μM to 100 μM at $q^2 = 1.4 \times 10^{11}$ m^{-2}) to examine whether the dimer-monomer equilibrium is indeed negligible in the resting or dark state. Because the intensity of the TG diffusion signal primarily reflects the number of dissociative molecules (dimers), intensity is a good indicator of dimer population. When the observed signals were normalized to the thermal grating intensity, an indicator of photoexcited protein levels, we found that the intensity of the diffusion peak was independent of concentration. We therefore conclude that UVR8 exists exclusively as a dimer in the absence of UV-B and protein partner, at least in the concentration range of our measurements. (Indeed, by using a size exclusion chromatography, it was found that the dimeric form is dominant in the dark state even at smaller concentrations than those for the TG measurements.)

The UVR8 monomer possesses 10 Trp residues in addition to the 4 that comprise the cross-dimer Trp-pyramid. One possible reason for this high Trp content is that photoexcitation of multiple Trp residues is required for the dissociation reaction. Traditional biochemical approaches using continuous UV-B irradiation cannot fully address this point. To further investigate this possibility, we measured the pulsed-light induced TG signals at various excitation light intensities. The number of reactive molecules, which is proportional to the square root of the amplitude of the molecular diffusion signal, was plotted against the excitation laser intensity (Fig. 3). If multi-photon excitation was required for the dissociation reaction, the number of dissociated molecules should have increased nonlinearly with the power of the excitation beam. As shown

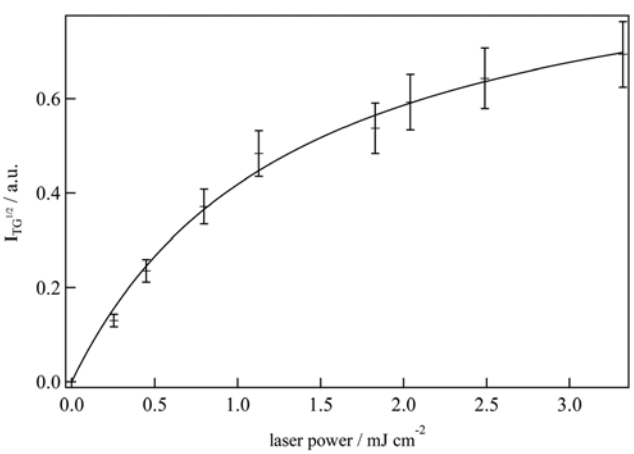

Fig. 3 Excitation light intensity dependence of the square root of transient grating signal intensity, which is proportional to reaction yield. The solid line is a fitted curve based on one-photon excitation (with a saturation effect).

in Fig. 3, however, TG signal intensity increased linearly with increasing light intensity over the range of relatively weak light intensities, indicating that multi-photon excitation was not needed for the dissociation reaction. At strong light intensities, the number of dissociated molecules plateaued, which can be explained simply by the saturation effect of the excitation.

3.3. Mutational analysis of the Trp-pyramid

As demonstrated above, the efficiency of the UVR8 photoreaction could be monitored quantitatively by measuring the TG diffusion signal intensity. Taking advantage of this relationship, we investigated the efficiency of the reaction in several mutants associated with the Trp-pyramid (W94F, W233F, W285F, and W337F) to identify the most important residues in the dissociation process. CD spectra of some Trp mutants have been reported previously.[13] Nevertheless, we measured CD spectra of several mutants to enable comparison under identical conditions (Fig. 4a). All generated CD spectra exhibited the exciton coupling effect reported previously.[13,40] The peak-to-trough signature reflects the splitting of the excited states into two components by the exciton coupling.[40] Because the coupling effect becomes stronger as the interactions between Trps are enhanced, the intensity of the CD spectra associated with the exciton coupling is a good indicator of the Trp-pyramid structure at the UVR8 dimer interface. The strongest exciton coupling was observed in the wild type (WT), followed in order by W337F, W285F, W94F, and W233F mutants. This decrease in CD intensity indicates that these Trps were indeed involved in the formation of the exciton couplet (Trp-pyramid). The relative strength of the exciton coupling also indicates that the WT formed the most compact Trp-pyramid structure. If structural integrity of the Trp-pyramid is related to enhanced efficiency of the dissociation reaction, the WT should show the highest yield of dissociation. We therefore examined this hypothesis using the TG method.

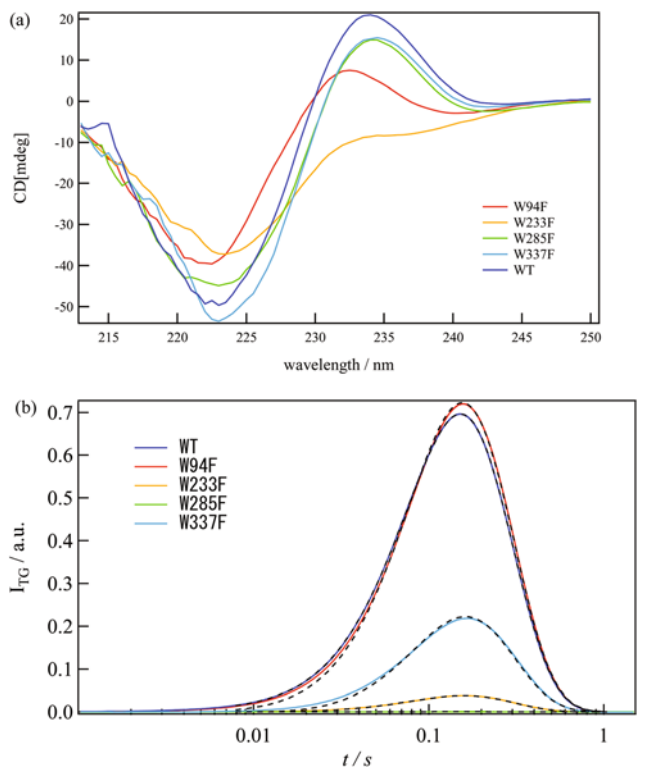

Fig. 4 (a) Circular dichroism (CD) spectra of wild-type (WT) protein and tryptophan mutants. The positive and negative peaks are indicative of exciton coupling. (b) Typical transient grating signals of 20 μM WT and tryptophan mutants at $q^2 = 1.4 \times 10^{11}$ m^{-2}.

The TG signals for the WT and Trp-pyramid mutants are shown in Fig. 4b. All mutants showed thermal grating and molecular diffusion signals similar to those of the WT. Peak intensities of the molecular diffusion signals significantly depended on the mutations (Fig. 4b). The intensity of the molecular diffusion signal reflects both the D_R to D_P ratio and the photoreaction quantum yield. If the D ratio is changed, the shape of the diffusion signal should change and the D-values obtained by curve-fitting should vary. When the signals were normalized relative to peak intensity, however, the temporal profiles were very similar to one another except for the very weak signal of W285F, which was noisy. The change in peak intensity was therefore attributed to changes in the reaction yield of dissociation. Peak intensities of the mutants, except for W94F, were smaller than that of the WT, indicating that W233, W285, and W337 residues (forming the base of the Trp-pyramid) are important to the photodissociation yield. The weakness of the W285F signal implies that W285 is the most important residue for photodissociation, even though the exciton coupling of W285F remained as strong as that of the WT, based on our CD measurements. This result indicates that photoexcitation of the exciton coupling itself is not directly proportional to the yield of the dimer dissociation reaction. The strength of the W94F TG signal indicates that W94 is not essential for the dissociation process. This result agrees with previous data showing that UV-B-induced monomerization still occurs when W94 is mutated, as observed by size exclusion chromatography.[13]

The above results demonstrate that W285 is a critical residue in the photodissociation of the UVR8 dimer. To more closely examine the underlying mechanism, the reaction dynamics of W285A were compared with those of W285F. Crystallographic studies have shown that W285 (and adjacent R286) lie within a pi-stack,[13] and that the structural integrity of the Trp-pyramid is more compromised in the W285A mutant than in W285F.[29] The TG signals of W285A and W285F mutants are shown in Fig. 5. The signals were fitted to a bi-exponential function (eqn (1)); the values of D_P and D_R obtained for W285A were identical to those of the WT, indicating that the observed D-change was due to the dimer dissociation reaction. The measured signal intensity thus represented the efficiency of the reaction. We initially speculated that the TG signal of W285F should be stronger than that of W285A, because phenylalanine (Phe) is an aromatic residue more bulky than alanine (Ala) and would be expected to form

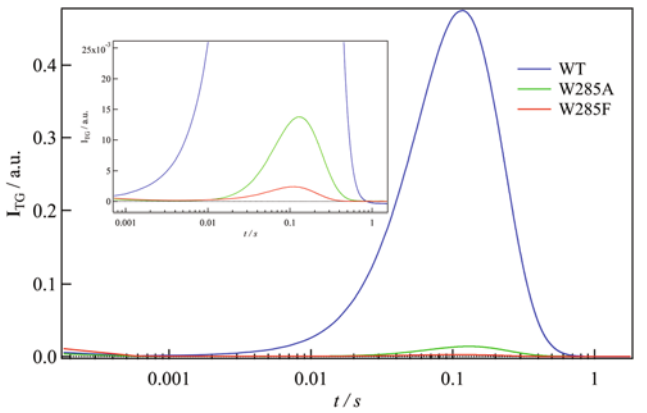

Fig. 5 Typical transient grating signals of 40 μM wild-type (WT) protein and W285 mutants at $q^2 = 1.4 \times 10^{11}$ m^{-2}. Inset: magnified view showing weak signals.

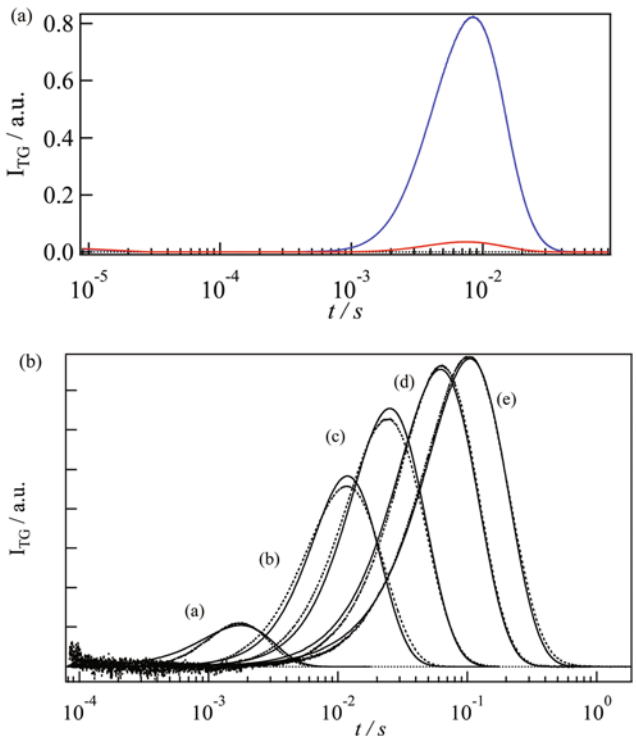

Fig. 6 (a) Typical transient grating signals of 20 μM wild-type protein (WT; blue line) and the monomer mutant R146A/R286A (red line) at $q^2 = 2.0 \times 10^{11}$ m^{-2}. The intensity of R146A/R286A was much lower than that of the WT. (b) The q^2-dependence of the transient grating signal (dotted lines) of R146A/R286A at 20 μM. The q^2-values were (a) 1.1×10^{13}, (b) 1.5×10^{12}, (c) 6.1×10^{11}, (d) 2.3×10^{11}, (e) 1.3×10^{11} m^{-2}. The signals were normalized to the thermal grating intensity. The best-fitted curves under a two-state model are shown as solid lines.

an exciton couplet with the other Trps. In addition, the crystal structure of W285F is similar to that of the WT, indicating that Phe substitution should be a less drastic mutation.[29] Our results, however, were the opposite of this expectation: W285A showed a stronger molecular diffusion signal than did W285F. This result may be explained in terms of the location of W285. According to the crystal structure of W285A, W233 leans toward the position of W285 because of the wider space generated by the replacement of Trp by Ala.[29] In the W285F mutant, on the other hand, the neighboring Trps cannot approach the W285 position because of the steric hindrance imposed by the aromatic side chain of Phe.[29] Hence, we conclude that the additional Trps close to the location of W285 are of structural importance.

3.4. Photoreactions of monomeric mutants

Our TG analysis demonstrated that the *D*-change of WT UVR8 not only reflected the dissociation reaction but also a conformational change. To further examine and clarify this conformational change, we investigated the reaction of several monomeric mutants to be able to subtract the contribution of the dissociation reaction from the TG signal. The dimer is stabilized mainly by electrostatic interactions (salt bridges) formed by residues R146 with E182, R286 with D96 and D107, and R338 with D44.[13] When these charged residues are replaced by uncharged residues such as Ala or asparagine, UVR8 loses its ability to form a dimer in the absence of UV-B.[13,29] The CD spectra of R146A/R286A, R338A, and D96N/D107N indicate that these proteins indeed exist as monomers, as they exhibited reduced exciton coupling.[13,29]

The temporal profile of the TG signal of R146A/R286A included both thermal and molecular diffusion components. As expected, the R146A/R286A molecular diffusion signal was very weak compared with that of the WT (Fig. 6a) because no *D*-change due to the dissociation reaction of the dimer was recorded. The diffusion signal (*i.e.*, rise and decay feature), on the other hand, revealed that a small *D*-change was induced even in the monomer unit. These findings indicate that the conformational change observed for WT UVR8 is also detectable in the monomer unit. To investigate the photoreaction dynamics, we measured the molecular diffusion signal under various q^2 conditions (Fig. 6b). The intensity of the diffusion signal was strongly dependent on q^2, and increased as the observation time range was lengthened from a few milliseconds to seconds. At longer times, at which point the *D*-change was nearly complete, D_P and D_R were determined to be 7.1×10^{-11} m^2 s^{-1} and 6.6×10^{-11} m^2 s^{-1}, respectively. Interestingly, D_P of R146A/R286A was the same as that of the WT, indicating that the final product had the same structure despite differences in the initial states. Although the TG signal of WT UVR8 was analyzed according to eqn (3), the molecular diffusion signals of the monomer mutants were well reproduced over a wide time range based on eqn (2) and (S-4).† This latter result is consistent with the fact that the dissociation reaction was not induced in the R146A/R286A monomer. D_I and k^{-1} were determined to be 6.6×10^{-11} m^2 s^{-1} and 3.4 ms, respectively.

We measured the CD spectrum of R146A/R286A under dark and light conditions. The CD spectrum did not change upon UV-B illumination, indicating that dissociation and

subsequent disruption of the exciton couplet was not induced in the monomer mutant. The absence of any detectable change in the CD spectrum also suggests that UV-B irradiation induced minimal secondary structural changes in R146A/R286A. We therefore concluded that the observed conformational change based on the TG measurement (a small increase in D) was due not to secondary structural changes, but was instead the result of an alteration in tertiary structure. Taking into account the fact that D was increased and that exposure of hydrophobic regions generally decreases friction because number of hydrogen bonds with surrounding water molecules decreases, we propose that this tertiary change was associated with the exposure of a hydrophobic region.

Although we observed a conformational change in the monomer unit, the time constant (3.4 ms) was significantly different from that of WT UVR8 (50 ms). We also measured and analyzed the TG signal of the R338A monomer mutant and obtained nearly identical results (D_R = 6.5 × 10^{-11} m^2 s^{-1}; D_I = 6.5 × 10^{-11} m^2 s^{-1}; D_P = 7.1 × 10^{-11} m^2 s^{-1}; k^{-1} = 5 ms).

To explain the different rates observed between the monomeric mutants and WT UVR8, we hypothesized that these monomeric mutants might influence the photochemistry of the Trp-pyramid because of their close proximity to the chromophore. To examine this possibility, we prepared an alternative monomeric mutant, D96N/D107N. The D96N/D107N mutant was chosen because its influence on the Trp-pyramid was negligible, as both aspartic acid residues were located far from the Trp cluster.[13,29] In the same manner as described above, we analyzed the q^2 dependence of the diffusion signal of D96N/D107N, which was reproduced with D_R = 6.3 × 10^{-11} m^2 s^{-1}, D_I = 6.3 × 10^{-11} m^2 s^{-1}, D_P = 7.1 × 10^{-11} m^2 s^{-1}, and k^{-1} = 50 ms. As expected, the time constant was identical to that of the conformational change observed in WT UVR8. This result strongly suggests that R286A and R338A mutations perturbed the local structure of the Trp-pyramid cluster.

3.5. Photoreactions in the absence of the C-terminus

After photodissociation, the activated monomeric form of UVR8 is thought to interact with its downstream signaling partner COP1. A conformational change in the C-terminal region of UVR8 has been previously suggested to be important for this interaction.[9] To determine any contributions of the C-terminus to the UVR8 photoreaction, we analyzed a ΔC mutant of UVR8 (1–383) lacking the C-terminus. TG signals of the WT and the ΔC mutant at various q^2 values are shown in Fig. 7. Although the molecular diffusion signal of the ΔC mutant decreased slightly in intensity compared with that of the WT, the time development of this signal was very similar in both forms of the protein. We analyzed the data according to the three-state model, which gave D and reaction rates of D_R = 6.1 × 10^{-11} m^2 s^{-1}, D_{I1} = 6.1 × 10^{-11} m^2 s^{-1}, D_{I2} = 6.7 × 10^{-11} m^2 s^{-1}, D_P = 8.3 × 10^{-11} m^2 s^{-1}, k_1^{-1} = 50 ms, and k_2^{-1} = 200 ms. These reaction rates were identical to those of the WT, indicating that the kinetics of both the initial conformational change and the dimer dissociation were not influenced by the presence or absence of the C-terminal region. This result demonstrates that the C-terminal region is not required for dimerization or UV-B-induced monomerization.

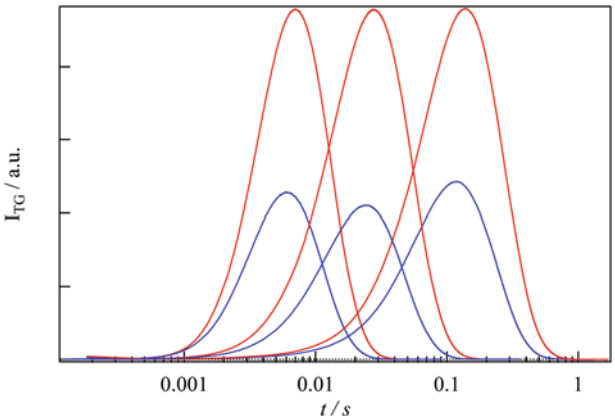

Fig. 7 Transient grating signals of the wild type (WT; red lines) and the ΔC mutant (blue lines) at q^2 = 2.6 × 10^{12}, 5.6 × 10^{11}, and 1.3 × 10^{11} m^{-2} (left to right). For comparison of intensities of the ΔC mutant, the signals were normalized relative to the peak intensities of the WT.

As expected for a truncation mutant, D_P and D_R of the mutant were larger than those of the WT, because the ΔC mutant had a smaller molecular size. Rough estimation of D based on molecular size (roughly proportional to the number of residues) using the Stokes–Einstein relationship, however, revealed that the increase in D due to removal of the C-terminal, D_R(ΔC mutant)/D_R(WT) = 1.17, was larger than its predicted value of approximately 1.05 (from $[440/383]^{1/3}$). This result indicates that the C-terminal region has highly extended structure and/or causes more friction due to strong intermolecular interaction with solvent. As reported previously, D-values of proteins having secondary structures (*e.g.*, α-helixes or β-sheets) are larger than those of identical proteins having unfolded secondary structures because intermolecular hydrogen bonding between proteins and water molecules causes large amounts of friction.[38,39] The C-terminal region may thus be considered to undergo intermolecular hydrogen bonding with water, suggesting a flexible structure. This conclusion is consistent with the fact that the C-terminal region disturbs the crystallization of UVR8.[13,29] The ratio of D_R to D_P of the ΔC mutant, 1.36, was almost identical to that of the WT (1.39). Although the small difference might reflect a conformational change within the C-terminal region, this result indicates that there is no drastic change in secondary structure of C-terminal region upon monomerization, which is consistent with the previous FTIR study in which the presence/absence of C-terminal region did not affect the light-minus-dark FTIR difference spectra significantly.[36]

4. Discussion

Considering the photochemistry inherent to Trps, photoexcitation of W285 could induce a Trp radical or cation. However,

even though the lifetime of the dissociated state of UVR8, as discussed below, was more than 13 hours, the absorption spectrum of the protein did not change in response to illumination. This result is not too surprising, because a Trp radical or cation formed by photoexcitation, could return to the ground state within micro- to milliseconds.[41] Hence, even if the dissociation was triggered by an electron transfer reaction involving W285, the radical or cation of the Trp residue is unlikely to be responsible for maintaining the monomeric state of UVR8. We therefore expect that residues within the Trp-pyramid (notably W285) might induce an electron transfer to another amino acid side chain, with the Trp involved immediately returning to the ground state by accepting an electron from the solvent or nearby residues. An electron-acceptor residue might maintain the monomeric state by destabilizing the intermolecular salt bridges at the UVR8 homodimeric interface.

One plausible electron acceptor capable of producing an intermediate that reverses very slowly would be a disulfide bond. In fact, photochemical reactions induced by near-UV light excitation of a Trp residue have been previously reported to lead to breakage of disulfide bridges.[41] UVR8 potentially has large conformational flexibility because N- and C-terminal regions are not linked directly within the same blade.[13] If the disulfide bridge is broken, UVR8 is considered to be consequently more flexible, possibly influencing the conformation of the dimer interface.

To test the possibility that disulfide bond recovery is a rate-limiting process for UVR8, we measured the recovery of CD spectra under deoxygenized conditions, with a nitrogen stream applied to prevent re-oxidation. CD spectra of UVR8 observed in darkness and following UV-B illumination under these conditions are shown in Fig. 8. Spectral characteristics obtained in the dark state represent the strong exciton coupling of the aromatic residues at the interface between the two monomers. CD spectral recovery under air-saturated conditions is shown in Fig. 8a. The time constant of the recovery was calculated from the time dependence of the signal intensity to be about 13 hours. When dissolved oxygen was purged, the CD spectral recovery rate was greatly slowed (Fig. 8b). This result suggests that recovery to the dimer requires oxidation of a reduced amino acid side chain.

The reported crystal structures of UVR8 have no disulfide bonds,[13,29] but were determined under reducing conditions in a synchrotron beam, which is also capable of reducing disulfide bonds. The location of cysteine (Cys) residues within the UVR8 structure suggests that a possible disulfide bond might be able to form between C127 and C132 (on adjacent β-strands of the third propeller blade) in close proximity to the Trp-pyramid. If these Cys residues formed a disulfide bond in the dark-state dimer, photo-electron transfer from W285 could break the disulfide bond, potentially increasing conformational flexibility between N-terminal blade 1 and C-terminal blade 7 of the propeller fold. As aspartic acids D96 and D107, which contribute to salt bridges important for dimerization, are located in adjacent blade 2, increased flexibility could disrupt

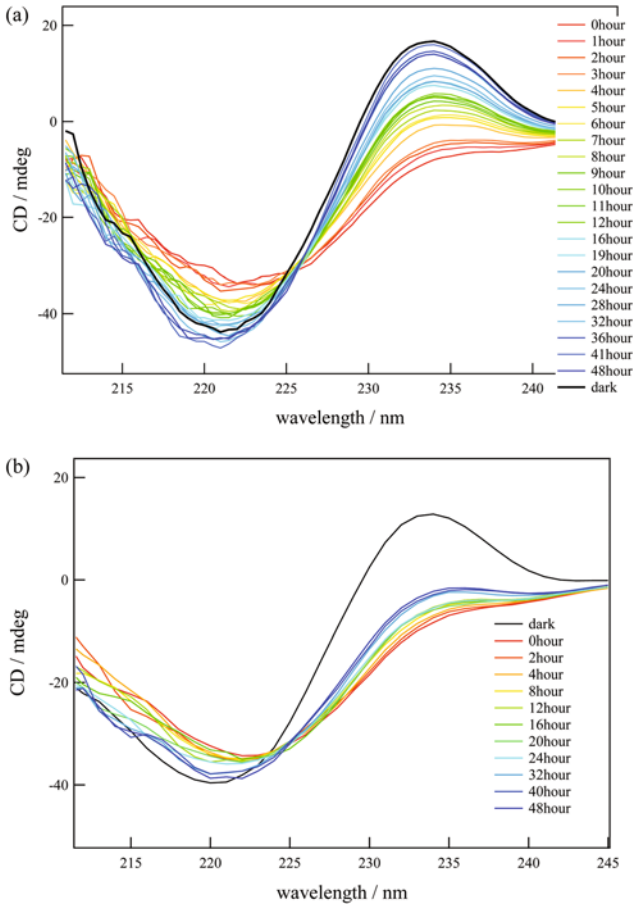

Fig. 8 Time dependence of circular dichroism (CD) spectra of non- or light-illuminated samples under (a) air-saturated and (b) oxygen-purged conditions.

these cross-dimer salt bridges to induce dissociation. The regeneration kinetics is accelerated *in vivo* in the presence of protein partner such as COP1, RUP1 and RUP2,[14,15] which may indicate that the flexibility is suppressed by the intermolecular interaction. In an initial test of this possibility, we generated a C132T mutant of UVR8, but SDS-PAGE measurements indicated that this mutant was dimeric (Fig. S1†). Thus, even if a disulfide bond forms between C127 and C132, it does not

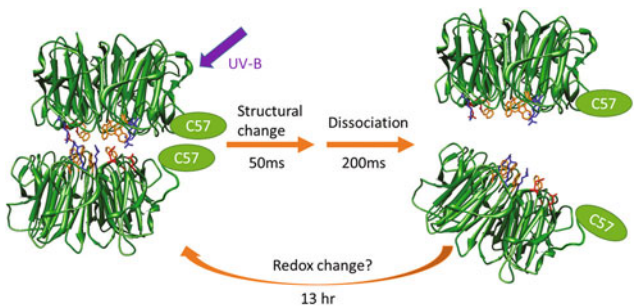

Fig. 9 Illustrated reaction scheme of UVR8.

appear to affect monomer-dimer status. Although we have not identified the electron acceptor, we nevertheless have demonstrated that the redox chemistry is a key factor contributing to the UVR8 oligomeric state. This point should be examined in future.

5. Conclusion

In this study, we investigated the photochemical reaction kinetics of UVR8 and specific mutants with respect to *D*, by using the pulsed laser-induced TG method. The UVR8 photodissociation reaction was found to proceed by three steps: photoexcitation of W285, an initial conformational change with a time constant of 50 ms, and dimer dissociation with a time constant of 200 ms. In addition, we determined that photoexcitation of a single residue, W285, is critical for the dissociation; Trp residues W337 and W233 also contribute, although less efficiently, to the reaction process. To detect the role of the C-terminal region, we investigated a Δ*C* mutant. Although the C-terminal region of UVR8 was reported to interact with the downstream signaling partner COP1, the photoreactions of WT UVR8 and the Δ*C* mutant were very similar; in particular, although the intensity of the molecular diffusion signal of the Δ*C* mutant was slightly decreased compared with that of the WT, the dissociation kinetics were almost the same. The ratio of D_R to D_P was slightly altered in the Δ*C* mutant (1.3 *vs.* 1.4 in the WT), which may indicate a C-terminal region conformational change. However, the very minor effect suggest that this C-terminal conformational change is minimal, at least *in vitro*.

A conformational change in the monomer was detected by the TG method in three monomeric mutants: R146A/R286A, R338A, and D97N/D106N. Although rate constants for the R146A/R286A and R338A mutants were slightly different from those of the WT, the D96N/D107N mutant exhibited rate constants matching the WT. Residues R286 and R338 were thus inferred to perturb the local structure of the Trp-pyramid cluster. Enhancement of diffusion signal intensity compared with that of D96N/D107N was also observed upon mutation of arginine residues (R146A/R286A and R338A).

To explain the existence of the long-lived active monomer state without any obvious change in the UVR8 absorption spectrum, we propose that UV-B sensing involves photo-electron transfer from W285. This possibility was tested by examining CD recovery under oxygen-purged conditions. Because the recovery rate was significantly reduced under oxygen-purged conditions, we suggest that redox reactivity is key to UVR8 dimeric state regeneration.

The reaction scheme of UVR8 is summarized in Fig. 9.

Acknowledgements

This work was supported by a Grant-in-Aid for Scientific Research (A) (no. 18205002), a Grant-in-Aid for Scientific Research on Innovative Areas (Research in a Proposed Research Area) (20107003 and 25102004) from the Ministry of Education, Culture, Sports, Science and Technology in Japan, an international collaboration program on UVR8 supported by the Japan Society for the Promotion of Science (to MT), and a grant from the National Science Foundation (1330856) Division of Molecular and Cellular Biosciences (to EDG).

References

1 B. A. Brown, C. Cloix, G. H. Jiang, E. Kaiserli, P. Herzyk, D. J. Kliebenstein and G. I. Jenkins, *Proc. Natl. Acad. Sci. U. S. A.*, 2005, **102**, 18225–18230.
2 J. J. Favory, A. Stec, H. Gruber, L. Rizzini, A. Oravecz, M. Funk, A. Albert, C. Cloix, G. I. Jenkins, E. J. Oakeley, H. K. Seidlitz, F. Nagy and R. Ulm, *EMBO J.*, 2009, **28**, 591–601.
3 K. Tilbrook, A. B. Arongaus, M. Binkert, M. Heijde, R. Yin and R. Ulm, *Arabidopsis Book*, 2013, vol. 11, p. e0164.
4 G. I. Jenkins, *Plant Cell*, 2014, **26**, 21–37.
5 M. Heijde and R. Ulm, *Trends Plant Sci.*, 2012, **17**, 230–237.
6 D. J. Kliebenstein, J. E. Lim, L. G. Landry and R. L. Last, *Plant Physiol.*, 2002, **130**, 234–243.
7 X. Huang, X. Ouyang, P. Yang, O. S. Lau, L. Chen, N. Wei and X. W. Deng, *Proc. Natl. Acad. Sci. U. S. A.*, 2013, **110**, 16669–16674.
8 L. Rizzini, J. J. Favory, C. Cloix, D. Faggionato, A. O'Hara, E. Kaiserli, R. Baumeister, E. Schafer, F. Nagy, G. I. Jenkins and R. Ulm, *Science*, 2011, **332**, 103–106.
9 C. Cloix, E. Kaiserli, M. Heilmann, K. J. Baxter, B. A. Brown, A. O'Hara, B. O. Smith, J. M. Christie and G. I. Jenkins, *Proc. Natl. Acad. Sci. U. S. A.*, 2012, **109**, 16366–16370.
10 X. Huang, P. Yang, X. Ouyang, L. Chen and X. W. Deng, *PLoS Genet.*, 2014, **10**, e1004218.
11 A. O'Hara and G. I. Jenkins, *Plant Cell*, 2012, **24**, 3755–3766.
12 Z. Liu, X. Li, F. W. Zhong, J. Li, L. Wang, Y. Shi and D. Zhong, *J. Phys. Chem. Lett.*, 2014, **5**, 69–72.
13 J. M. Christie, A. S. Arvai, K. J. Baxter, M. Heilmann, A. J. Pratt, A. O'Hara, S. M. Kelly, M. Hothorn, B. O. Smith, K. Hitomi, G. I. Jenkins and E. D. Getzoff, *Science*, 2012, **335**, 1492–1496.
14 M. Heijde and R. Ulm, *Proc. Natl. Acad. Sci. U. S. A.*, 2013, **110**, 1113–1118.
15 M. Heilmann and G. I. Jenkins, *Plant Physiol.*, 2013, **161**, 547–555.
16 C. Cloix and G. I. Jenkins, *Mol. Plant*, 2008, **1**, 118–128.
17 B. A. Brown and G. I. Jenkins, *Plant Physiol.*, 2008, **146**, 576–588.
18 G. I. Jenkins, *Annu. Rev. Plant Biol.*, 2009, **60**, 407–431.
19 J. J. Wargent, V. C. Gegas, G. I. Jenkins, J. H. Doonan and N. D. Paul, *New Phytol.*, 2009, **183**, 315–326.
20 B. A. Brown, L. R. Headland and G. I. Jenkins, *Photochem. Photobiol.*, 2009, **85**, 1147–1155.

21 H. Gruber, M. Heijde, W. Heller, A. Albert, H. K. Seidlitz and R. Ulm, *Proc. Natl. Acad. Sci. U. S. A.*, 2010, **107**, 20132–20137.
22 P. V. Demkura, C. L. Ballaré, C. L. Ballare and C. L. Ballaré, *Mol. Plant*, 2012, **5**, 642–652.
23 M. P. Davey, N. I. Susanti, J. J. Wargent, J. E. Findlay, W. Paul Quick, N. D. Paul and G. I. Jenkins, *Photosynth. Res.*, 2012, **114**, 121–131.
24 C. L. Ballaré, *Annu. Rev. Plant Biol.*, 2014, **65**, 335–363.
25 S. Singh, S. B. Agrawal and M. Agrawal, *J. Photochem. Photobiol., B*, 2014, **137**, 67–76.
26 R. Fasano, N. Gonzalez, A. Tosco, F. Dal Piaz, T. Docimo, R. Serrano, S. Grillo, A. Leone, D. Inzé and D. Inze, *Mol. Plant*, 2014, **7**, 773–791.
27 V. Tossi, L. Lamattina, G. I. Jenkins and R. O. Cassia, *Plant Physiol.*, 2014, **164**, 2220–2230.
28 S. Hayes, C. N. Velanis, G. I. Jenkins and K. A. Franklin, *Proc. Natl. Acad. Sci. U. S. A.*, 2014, **111**, 11894–11899.
29 D. Wu, Q. Hu, Z. Yan, W. Chen, C. Yan, X. Huang, J. Zhang, P. Yang, H. Deng, J. Wang, X. Deng and Y. Shi, *Nature*, 2012, **484**, 214–219.
30 D. J. Kliebenstein, J. E. Lim, L. G. Landry and R. L. Last, *Plant Physiol.*, 2002, **130**, 234–243.
31 M. Heijde, M. Binkert, R. Yin, F. Ares-Orpel, L. Rizzini, E. Van De Slijke, G. Persiau, J. Nolf, K. Gevaert, G. De Jaeger and R. Ulm, *Proc. Natl. Acad. Sci. U. S. A.*, 2013, **110**, 20326–20331.
32 L. Rizzini, J.-J. J. Favory, C. Cloix, D. Faggionato, A. O'Hara, E. Kaiserli, R. Baumeister, E. Schäfer, F. Nagy, G. I. Jenkins, R. Ulm, E. Schafer, F. Nagy, G. I. Jenkins and R. Ulm, *Science*, 2011, **332**, 103–106.
33 M. Wu, A. Strid, L. A. Eriksson, Å. Strid and L. A. Eriksson, *J. Phys. Chem. B*, 2014, **118**, 951–965.
34 X. Li, L. W. Chung, K. Morokuma and G. Li, *J. Chem. Theory Comput.*, 2014, **10**, 3319–3330.
35 A. A. Voityuk, R. A. Marcus and M.-E. E. Michel-Beyerle, *Proc. Natl. Acad. Sci. U. S. A.*, 2014, **111**, 5219–5224.
36 M. Heilmann, J. M. Christie, J. T. M. Kennis, G. I. Jenkins and T. Mathes, *Photochem. Photobiol. Sci.*, 2014, **14**, 252–257.
37 M. Terazima, *Phys. Chem. Chem. Phys.*, 2011, **13**, 16928–16940.
38 M. Terazima, *Biochim. Biophys. Acta*, 2011, **1814**, 1093–1105.
39 M. Terazima, *Phys. Chem. Chem. Phys.*, 2006, **8**, 545–557.
40 I. B. Grishina and R. W. Woody, *Faraday Discuss.*, 1994, **99**, 245–262.
41 M. T. Neves-Petersen, S. Klitgaard, T. Pascher, E. Skovsen, T. Polivka, A. Yartsev, V. Sundstrom and S. B. Petersen, *Biophys. J.*, 2009, **97**, 211–226.

